

Interbeat Interval Detection from Synthetic Photoplethysmography Signals

Clémentine Aguet^{1,2}, Loïc Jeanningros^{1,2}, Fabian Braun¹, Jérôme Van Zaen¹, Mathieu Lemay¹

¹Swiss Center for Electronics and Microtechnology (CSEM), Neuchâtel, Switzerland

²Ecole Polytechnique Fédérale de Lausanne (EPFL), Lausanne, Switzerland

Abstract

With the increased presence of wearables, photoplethysmography (PPG) is a promising alternative to electrocardiography (ECG) for the monitoring of physiological parameters related to cardiovascular diseases. However, the evaluation of PPG-based methods is more challenging since PPG signals are less frequently available in databases compared to ECG signals.

Generative adversarial networks (GANs) are a promising alternative to synthesize PPG signals and compensate for unavailable PPG recordings. We propose a modified GAN architecture to generate PPG signals from a sequence of spikes located at R-peak positions of the ECG. The validity of the synthetic PPG signals was evaluated in two ways. First, by comparing the statistical distribution of the pulse wave morphology features of real vs. synthetic PPGs. Second, by comparing the interbeat-intervals (IBIs) of the synthetic PPGs vs. the ECG-based reference IBIs.

The statistical distributions did not reveal significant difference between real and synthetic PPGs. In addition, the IBIs extracted from synthetic PPGs were accurately reproducing the ECG-based reference IBIs, with a mean absolute error of 10.24 ms. Overall, the results highlight the potential of synthetic PPG to optimize and validate PPG-based method for cardiovascular monitoring.

1. Introduction

Electrocardiography (ECG) measures the electrical activity of the heart. It is a widespread method for monitoring the cardiac health and performing cardiac function analysis. In contrast, photoplethysmography (PPG) is an optical technique to assess blood volume variations in the microvascular bed of tissues. Such a convenient, low-cost and non-invasive technology can easily be embedded in wearable devices. Therefore, there has been a growing interest in using PPG as an alternative to ECG for the monitoring of various physiological parameters related to cardiovascular diseases [1]. Among those parameters, heart rate variability (HRV) is a good

indicator of cardiac health and helps to understand the regulation of the cardiac activity by the autonomic nervous system. The HRV analysis is conventionally based on RR intervals obtained from an ECG recording. By analogy, the interbeat intervals (IBIs) can be extracted from PPG signals to retrieve pulse rate variability information as surrogate of HRV [2].

The development of models to monitor such parameters generally requires large databases for optimization and evaluation. The availability of data can become a critical limitation. Although essential, collecting and annotating large amount of data is a difficult and costly process, especially for healthcare applications. Due to the ease of access to public databases with annotated ECG recordings, the monitoring of cardiovascular parameters is usually performed with ECG-based methods. Unlike ECG, it is less common to have access to large databases with PPG recordings. Consequently, a thorough optimization and evaluation of PPG-based methods is more difficult.

To overcome this issue, we propose a model based on generative adversarial networks (GANs) to artificially generate PPG signals from ECG data. The main challenge with synthetic PPGs is not only to synthesize signals with realistic-looking waveform morphology but also to preserve their physiological properties and their temporal consistency with the ECG signal. For the evaluation of the proposed method, we first quantified the similarity between GAN-synthetic vs real PPG signals by comparing the statistical distribution of pulse wave morphology features. Additionally, we validated the temporal consistency of the synthetic PPG signals with respect to the ECG signal using a PPG-based IBI detection.

2. Materials and Methods

2.1. Dataset

The proposed model was trained and evaluated on a database collected at the University Hospital of Bern (Bern, Switzerland). The study was approved by the local ethics committee and registered at ClinicalTrials.gov (NCT03823105). The database includes signals from 1-lead ECG and from a proprietary, wrist-worn PPG device

[3]. 69 adult subjects were recorded, with both healthy volunteers and patients with sleep disorders.

2.2. Data Preprocessing

The PPG signal was filtered with high- and low-pass Butterworth filter to reduce noise and remove baseline drift. Two methods were then used to eliminate outliers. The first one detected the IBIs corrupted by motion using wrist-based accelerometer signals. The second used a Hampel filter which is based on the median absolute deviation. The PPG and ECG signals were aligned using dynamic time wrapping (DTW) on 30-minute windows. From the ECG signal, a sequence of spikes located at the R-peaks was created. The PPG was normalized within the range [0, 1]. Finally, the signal was split into non-overlapping 10-second windows.

2.3. Generative Adversarial Network

We developed a GAN architecture to generate a PPG signal from a sequence of spikes derived from the ECG R-peaks. This cross-modality signal-to-signal translation approach is based on CycleGAN [4]. The model takes as input a 10-second spike sequence and generates the corresponding PPG signal. Its architecture is illustrated in Figure 1. Two generators were implemented. $G_{PPG}: Spike \rightarrow PPG$ for the forward mapping and $G_{Spike}: PPG \rightarrow Spike$ for the backward mapping. Synthetic signals are denoted $PPG' = G_{PPG}(Spike)$ and $Spike' = G_{Spike}(PPG)$. Their architecture was based on UNet [5], with additional skip connections to help against vanishing gradient. Two discriminators were used to differentiate synthetic from real data ($D_{PPG}: PPG' \text{ vs. } PPG$ and $D_{Spike}: Spike' \text{ vs. } Spike$). The discriminators had the architecture of typical convolutional neural networks for a binary classification task. The cycle training is finalized by giving PPG' and $Spike'$ as inputs to G_{Spike} and G_{PPG} , respectively.

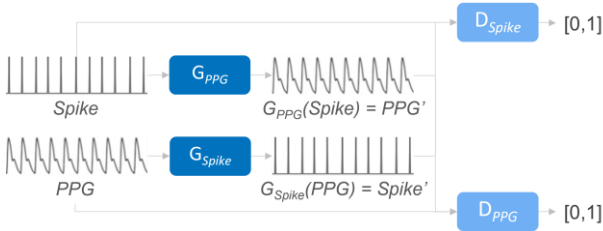


Figure 1. Architecture of the GAN.

The adversarial loss (\mathcal{L}_{adv}) commonly used in GANs was applied to both forward and backward mappings. In addition, CycleGAN introduced the cycle consistency loss function (\mathcal{L}_{cycle}) [4]. This second component imposes constraints on the generators and rewards the consistency of forward and backward mappings, meaning that

$G_{PPG}(G_{Spike}(p)) = p$ and $G_{Spike}(G_{PPG}(s)) = s$. The last component of the cost function is the identity loss ($\mathcal{L}_{Identity}$), which favors identity mapping and feature preservation. When a signal is given as input to the opposite generator, the output is expected to be the same as the input.

The GAN parameters were optimized with the Adam algorithm and learning rates set to 0.0002. The model was trained over 100 epochs with a batch size of 128. The hyperparameters were defined based on a literature review and experimentally adapted. The weights were initialized using a normal distribution. The overall model was implemented in Python using the *PyTorch* deep learning framework.

2.4. Evaluation

The evaluation of the proposed model was performed in two steps, further described in the following subsections. The first assessed the reliability of the PPG pulse wave morphology, while the second focused on the temporal consistency with the reference ECG signal. The evaluation was conducted on 50000 synthetic signals of 10-seconds.

2.4.1. PPG Pulse Wave Morphology

The main challenge with PPG is not only to synthesize realistic-looking signals but to preserve its physiological properties. To validate the similarity between synthetic and real PPG, the first evaluation was based on some known PPG pulse wave morphology features. It included the timings and amplitudes of the maximum of the first derivative (d_{max}) and the systolic peak ($syst$), all relative to the pulse foot ($foot$) (Figure 2)[6]. To compare their distributions and assess the similarity between real and synthetic data, we computed the Wasserstein distance.

2.4.1. Interbeat-Intervals

The second evaluation step was based on IBIs and aimed to assess the temporal consistency of the synthetic PPG sequences with respect to the ECG signal. A PPG-based IBI detection algorithm was separately applied to the real and synthetic PPG signals. This algorithm is based on the maximum of the PPG derivative. The reference IBI were obtained from the R-peaks in the ECG detected using the curvature of the signal.

The extracted IBIs were then compared to the values derived from the corresponding ECG, using the mean absolute error (MAE). First, we defined an interval (I) around each PPG beat time, defined as the maximum of the first derivative. It is delimited by the vertical dashed lines in Figure 2 and defined as:

$$I = \left[\frac{t_{PPGi-1} + t_{PPGi}}{2}, \frac{t_{PPGi} + t_{PPGi+1}}{2} \right]$$

When no ECG beat could be associated with I , the PPG beats were considered as false positives. And when multiple ECG beats were associated with I , they were considered as false negatives, except for the one ECG beat closest to the PPG beat. Then, the MAE was computed between PPG-IBIs (excluding false positives) and ECG-IBIs (excluding false negatives).

$$MAE = \mathbb{E}_i[\|IBI_{PPG_i} - IBI_{ECG_i}\|_1]$$

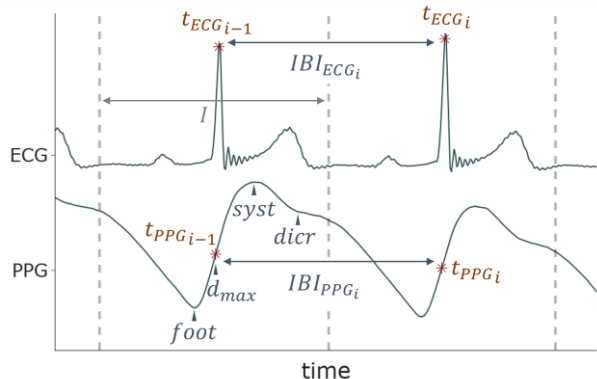


Figure 2. Interbeat interval (IBI) and pulse wave morphology features. t_{ECG_i} corresponds to the R-peak in the ECG signal. t_{PPG_i} is PPG beat time, defined as maximum of the derivative.

3. Results

Figure 3 shows three examples of the model outputs. This figure illustrates how the model can generate PPG signals with not only realistic-looking pulse waveform but preserved temporal consistency with ECG signals.

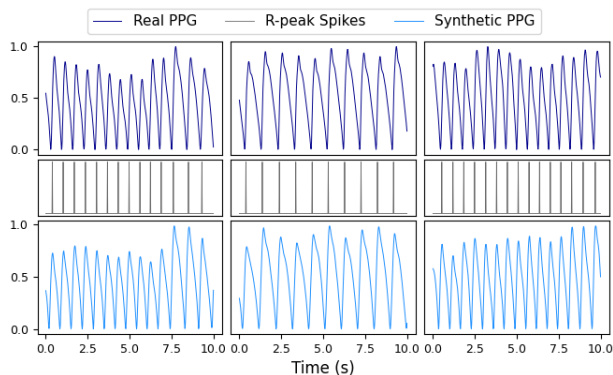


Figure 3. Three example of model input and output. (Top) Real PPG used to train the model. (Middle) Spike sequence from ECG R-peaks given as input. (Bottom) Synthetic PPG.

3.1. Pulse Wave Morphology Features

Statistical distributions of pulse wave morphology features comparing real and synthetic data are shown in Figure 4 and a visual inspection reveals a high similarity. To obtain a more quantitative idea of this comparison, the Wasserstein distance was computed, and the results are

presented in Table 1. The Wasserstein distance is small (<0.02) for all features. This aspect is consistent with the observation on statistical distributions previously mentioned. Overall, both the statistical distributions and the Wasserstein distance showed a similar variability of PPG waveform between real and synthetic data in terms of pulse wave morphology features.

Table 1. Similarity of the PPG pulse wave morphology features.

Features	Wasserstein distance
Time maximum derivative	0.0070
Amplitude maximum derivative	0.0008
Time systole	0.0134
Amplitude systole	0.0105

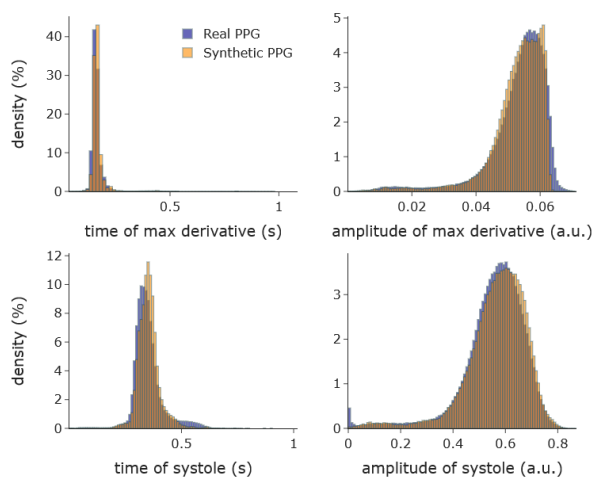


Figure 4. Statistical distributions of PPG pulse wave morphology features, comparing real and synthetic data. The timing and amplitude of the maximum of the first derivative and systolic peak.

3.2. IBI Detection

The PPG-based IBI extraction algorithm was evaluated against the reference ECG. The results for real and synthetic data are shown in Table 2 and Figure 5. PPG-based IBIs appear to be temporally consistent with respect to ECG-based IBIs, driving the generation process. Indeed, the MAE of synthetic PPG-based IBIs is slightly greater (10.24 ms) than of real PPG-based IBIs (7.00 ms). Detecting IBIs in real PPG signals is prone to some errors, we observe numerous outliers (up to 240 ms) in the MAE distribution (not shown Figure 5), as well as some false positive and false negative detections (Table 2). By contrast, synthetic PPG-based IBIs are slightly less accurate, but we observe a much lower number of outliers, as well as fewer false negatives and false positives.

Table 2. IBI detection statistics.

	Real PPG	Synthetic PPG
False positive (%)	0.26	0.04
False negative (%)	0.10	0.04
Mean absolute error (ms)	7.00	10.24
Std absolute error (ms)	6.71	7.23
Median absolute error (ms)	3.47	9.13

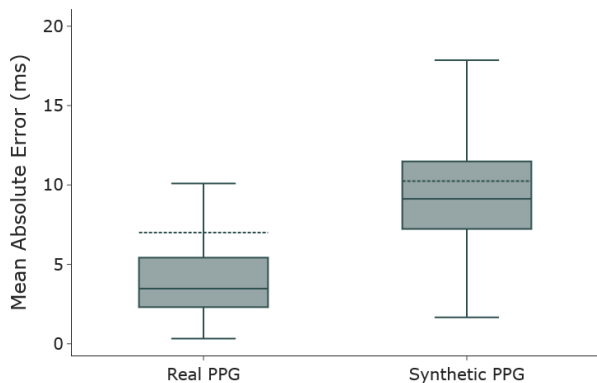


Figure 5. Mean Absolute Error between IBIs from ECG and from PPG (outliers are not shown). The dashed line corresponds to the mean value and the solid line the median.

4. Discussion

The evaluation of synthetic data is one of the biggest challenges when dealing with GANs, especially in presence of time-series rather than images. Our first approach was based on PPG pulse wave morphology features. It revealed the model capability to synthesize realistic-looking PPG signals with physiological pulse wave morphology. Nevertheless, the proposed model remains highly dependent on the data used for training and the variability of the synthetic pulse waveforms will not be greater than in real data. In a second evaluation step, the temporal consistency with respect to the ECG signal was assessed by comparing PPG-based IBI detection algorithm to the reference ECG. It also revealed that the synthetic PPG signals are less noisy than real PPG. This aspect is not surprising as GANs will focus on the significant trends of the data rather than noise. One limitation of the aforementioned evaluation methods is the dependence on the precise detection of some pulse wave morphology features (d_{max} and $syst$). Inaccuracy of the detection algorithm could strongly impact the evaluation of synthetic data. More complex features might be of interest for a deeper evaluation of the PPG pulse wave morphology. More particularly the dicrotic notch, as well as some characteristic points of the PPG second derivative. This will be the focus of a future work.

Besides the encouraging results, further investigations on the model itself could even improve the outcomes. First and as previously mentioned, the model hyperparameters were initialized based on literature review. However, a proper hyperparameter tuning could be beneficial for the

model training and the resulting performances. Another idea would be to guide the learning process with some important characteristic points of the PPG pulse waveform and its derivatives. This could ensure the generation of pulses with such points in physiological range. Finally, the length of the synthetic PPG signals was limited to 10 seconds, an increase of this sequence length could be particularly useful in the context of HRV analysis. This aspect will probably be the first to investigate.

5. Conclusion

The results of this study highlight the potential of GANs to artificially generate PPG signals. The proposed GAN architecture seems capable of learning to generate PPG signal with physiological waveform morphology. Furthermore, our model was able to generate PPG signals preserving a temporal consistency with the ECG R-peak sequence. This could help in optimizing and validating PPG-based methods for the monitoring of cardiovascular parameters via data augmentation.

References

- [1] M. Lemay *et al.*, “Applications of Optical Cardiovascular Monitoring,” in *Wearable Sensors (Second Edition)*, E. Sazonov, Ed. Oxford: Academic Press, 2021, pp. 487–517.
- [2] A. Schäfer and J. Vagedes, “How accurate is pulse rate variability as an estimate of heart rate variability?: A review on studies comparing photoplethysmographic technology with an electrocardiogram,” *International Journal of Cardiology*, vol. 166, no. 1, pp. 15–29, Jun. 2013.
- [3] F. Braun *et al.*, “Pulse Oximetry at the Wrist During Sleep: Performance, Challenges and Perspectives,” in *2020 42nd Annual International Conference of the IEEE Engineering in Medicine & Biology Society (EMBC)*, Montreal, QC, Canada, Jul. 2020, pp. 5115–5118.
- [4] J.-Y. Zhu, T. Park, P. Isola, and A. A. Efros, “Unpaired Image-to-Image Translation Using Cycle-Consistent Adversarial Networks,” in *2017 IEEE International Conference on Computer Vision (ICCV)*, Oct. 2017.
- [5] O. Ronneberger, P. Fischer, and T. Brox, “U-Net: Convolutional Networks for Biomedical Image Segmentation,” *arXiv:1505.04597 [cs]*, May 2015, Accessed: Aug. 26, 2021. [Online].
- [6] M. Proença *et al.*, “Pulse Wave Analysis Techniques,” in *The Handbook of Cuffless Blood Pressure Monitoring: A Practical Guide for Clinicians, Researchers, and Engineers*, J. Solà and R. Delgado-Gonzalo, Eds. Cham: Springer International Publishing, 2019, pp. 107–137.

Address for correspondence:

Clémentine Aguet
 CSEM SA
 Rue Jaquet-Droz 1, 2002 Neuchâtel, Switzerland
 clementine.aguet@csem.ch